

# Synthesis, magnetic property and DNA cleavage behavior of a new dialkoxo-bridged diiron(III) complex

Jing-Yuan Xu<sup>1,2</sup>, Jin-Lei Tian<sup>1</sup>, He-Dong Bian<sup>1</sup>, Shi-Ping Yan<sup>1\*</sup>, Dai-Zheng Liao<sup>1</sup>, Peng Cheng<sup>1</sup> and Pan-Wen Shen<sup>1</sup>

<sup>1</sup> College of Chemistry, Nankai University, Tianjin 300071, People's Republic of China

<sup>2</sup> College of Pharmacy, Tianjin Medical University, Tianjin 300070, People's Republic of China

Received 15 August 2006; Revised 17 November 2006; Accepted 1 December 2006

A new dialkoxo-bridged diiron(III) complex,  $[\text{Fe}_2(\text{BMA})_2(\text{CH}_3\text{O})_2\text{Cl}_2] \cdot 2\text{Cl} \cdot 4\text{CH}_3\text{OH}$  (**1**) [BMA = *N,N*-bis(2-benzimidazolylmethyl)amine], was synthesized and characterized by UV-visible absorption and infrared spectra and magnetic susceptibilities. The complex crystallizes in the monoclinic system, space group  $\text{P}2(1)/n$ ,  $a = 12.9659(19) \text{ \AA}$ ,  $b = 10.0278(16) \text{ \AA}$ ,  $c = 17.919(2) \text{ \AA}$ ,  $\beta = 93.766(8)^\circ$ ,  $V = 2324.8(6) \text{ \AA}^3$ ,  $Z = 2$ ,  $F(000) = 1036$ ,  $D_c = 1.426 \text{ g cm}^{-3}$ ,  $\mu = 0.908 \text{ mm}^{-1}$ . According to X-ray crystallographic studies, each Fe(III) ion lies in a highly distorted octahedral environment, and two Fe(III) ions are bridged by the methoxyl oxygens. Cryomagnetic analyses indicated a moderate antiferromagnetic interaction between the high-spin Fe(III) ions, with  $J = -27.05 \text{ cm}^{-1}$ . Moreover, the binding interaction of DNA with the diiron complex was investigated by spectroscopic and agarose gel electrophoretic methods, showing moderate cleavage activity on pBR322 plasmid DNA at physiological pH and temperature. Copyright © 2007 John Wiley & Sons, Ltd.

**KEYWORDS:** diiron(III) complex; crystal structure; magnetism; DNA cleavage; gel electrophoresis

## INTRODUCTION

Oxygen-bridged binuclear complexes have been of considerable interest for several decades, in relation to magnetic superexchange studies.<sup>1,2</sup> Additionally, special attention has been paid to oxygen-bridged diiron(III) complexes, mainly stimulated by the discovery of the Fe–O–Fe core in the active sites of a number of metalloproteins.<sup>3–11</sup> On the other hand, the DNA backbone is formed by phosphodiester links, ubiquitous chemical bonds in biological systems. Enzymes that hydrolyze phosphodiester bonds frequently possess catalytic metal ions in their active sites and the metal ions most frequently employed are  $\text{Mg}^{2+}$ ,  $\text{Zn}^{2+}$ ,  $\text{Fe}^{2+}$ ,  $\text{Mn}^{2+}$  and  $\text{Ca}^{2+}$ .<sup>12–17</sup> Thus the search for small metal complexes which are capable of catalytically hydrolyzing deoxyribonucleic acid

(DNA) is understandable; however it is also exceedingly difficult due to the resistance of DNA to hydrolysis.<sup>18</sup> Metal complexes are well established as phosphodiester cleavage agents and in general their action is mediated by a powerful nucleophilic attack.<sup>19–21</sup> These compounds have been demonstrated to be very useful as footprinting agents, probes for conformational variability of nucleic acids, as well as targeted nuclease activity.<sup>22,23</sup> Recently, we began to explore the nuclease activity of the complexes containing transition metal ions and various pyridyl- or imidazolyl-based ligands. In this work, we demonstrate that the new dinuclear  $[\text{Fe}_2(\text{BMA})_2(\text{CH}_3\text{O})_2\text{Cl}_2] \cdot 2\text{Cl} \cdot 4\text{CH}_3\text{OH}$  complex is able to cleave DNA through a possible hydrolytic mechanism under mild temperature and pH conditions, and exhibits moderate antiferromagnetic behavior.

\*Correspondence to: Shi-Ping Yan, College of Chemistry, Nankai University, Tianjin 300071, People's Republic of China.  
E-mail: yansp@nankai.edu.cn

Contract/grant sponsor: National Natural Science Foundation of China; Contract/grant number: 20331020.

Contract/grant sponsor: Tianjin Natural Science Foundation, China; Contract/grant number: 06YFJMJ12700.

Contract/grant sponsor: Tianjin University Committee Science Foundation, China; Contract/grant number: 20020106.

## EXPERIMENTAL SECTION

### Materials and equipment

Plasmid pBR322 DNA was purchased from Sino-American Biotechnology. All other starting materials were obtained from commercial suppliers and were of AR grade. BMA

ligand was synthesized by a published procedure.<sup>24</sup> Elemental analyses (C, H, N) were performed on a Perkin-Elmer 240 analyser. IR spectra were recorded on a Shimadzu IR-408 spectrometer as KBr pellets, and UV-vis spectra on a Shimadzu UV-2101PC UV-vis scanning spectrophotometer. Variable-temperature magnetic susceptibilities over 4.2–300 K were measured on a Maglab 2000 vibrating sample magnetometer. Agarose gel electrophoretic was performed on a Beijing Six-One DYY-2C electrophoresis instrument.

### Synthesis of complex 1

A methanol solution (15 ml) of BMA ligand (0.139 g, 0.5 mmol) was added dropwise to a methanol solution (15 ml) of  $\text{FeCl}_3 \cdot 2\text{H}_2\text{O}$  (0.100 g, 0.5 mmol). The mixture was stirred under reflux for 3 h and then left to cool down. The small amount of red precipitate formed was filtered and the resulting red solution was allowed to stand at room temperature. After 2 weeks, red well-shaped prismatic crystals were obtained, and many of them were suitable for X-ray diffraction studies. Yield: *ca* 70%. Anal. calcd for  $\text{C}_{38}\text{H}_{52}\text{Cl}_4\text{Fe}_2\text{N}_{10}\text{O}_6$ : C 45.71, H 5.25, N 14.03%. Found: C 45.56, H 5.22, N 14.19%.

### X-ray crystallography

Red prismatic crystal ( $0.35 \times 0.25 \times 0.20$  mm) was selected and mounted on a Bruker Smart 1000 diffractometer with graphite monochromatized  $\text{MoK}\alpha$  radiation ( $\lambda = 0.71073$  Å), using  $\omega$  scan technique at 293(2) K. A total of 4696 unique reflections ( $R_{\text{int}} = 0.0502$ ) were measured in the range of  $2.00^\circ \leq \theta \leq 26.39^\circ$ . The structure was solved by the direct method and successive Fourier difference synthesis, and refined by the full-matrix least-squares method on  $F^2$  with anisotropic thermal parameters for all non-hydrogen atoms.<sup>25</sup> Hydrogen atoms were generated geometrically and refined isotropically. A total of 273 parameters were refined. The final refinement converged at  $R_1 = 0.0536$ ,  $wR_2 = 0.1157$  for 2878 observed reflections with  $I \geq 2\sigma(I)$ , and  $R_1 = 0.1052$ ,  $wR_2 = 0.1346$  for all data with  $\text{GOF} = 1.010$ . The largest difference peak and hole were 0.671 and  $-0.583 \text{ e } \text{\AA}^{-3}$ , respectively.

### UV-visible absorption spectra for DNA binding study

The spectra of complex 1 in the absence of DNA were recorded in 10 mM pH 7.5 Tris-Cl buffer as a reference group. The absorption spectra of the diiron complex in the presence of DNA were measured after incubating their mixtures in 10 mM pH 7.5 Tris-Cl buffer for 10 min at 37 °C, where controlling the corresponding DNA solutions with increasing molar concentration ratio to complex 1 from 0:1 to 12:1 (DNA:complex 1).

### Electrophoretic assay for cleavage activity study

#### Preparation of agarose gel electrophoresis

Agarose gel (0.7% w/v) in  $1 \times$  TAE buffer (121 g Tris base, 18.6 g  $\text{Na}_2\text{EDTA}$  and 28.55 ml glacial acetic acid are dissolved

in the sterilized distilled water to 500 ml volume, thus constituting  $50 \times$  concentrate) was prepared. Then to 18  $\mu\text{l}$  of each of the incubated complex-plasmid mixtures was added 2  $\mu\text{l}$  tracking dye (50 mM Tris, 0.25% bromophenol blue and 50% glycerol), it was loaded onto the gel and the electrophoresis was carried out under TAE buffer system at 80 V for about 3 h, which was then transferred into the dye solution containing several drops of 0.5  $\mu\text{g}/\text{ml}$  ethidium bromide in  $1 \times$  TAE for half an hour. At the end of these processes, the gel was visualized under UV light using the BIO-Rad Trans illuminator IEC 1010. The illuminated gel was photographed with a Polaroid camera (a red filter and Polaroid type of film were used).

### pBR322 DNA cleavage experiments by complex 1

The complex solutions were prepared in DMSO with the concentrations of 5.00, 2.50, 1.25, 0.25 and 0 mM. Solution of pBR322 plasmid DNA (0.4 mg/ml) in the TE-buffer consisting of 1 mM Tris-HCl at pH 7.5, 1 mM NaCl and 1 mM EDTA as supplied, and sterilized distilled water as solvent, were used. Appropriate concentrations of the complex DMSO solution (4  $\mu\text{l}$ ) were added to 2  $\mu\text{l}$  of plasmid DNA and the total volume was made up to 18  $\mu\text{l}$  by adding TE buffer so that the concentration of DNA remained unchanged at 0.04 mg/ml while that of the complex was changed to 1.00, 0.50, 0.25, 0.05 and 0.00 mM corresponding to lanes 1–5. The mixtures were then incubated at 37 °C for 3 h.

## RESULTS AND DISCUSSION

### Crystal structure of complex 1

The structure of 1 consists of the binuclear cation  $[\text{Fe}_2(\text{BMA})_2(\text{CH}_3\text{O})_2\text{Cl}_2]^{2+}$ , two uncoordinated  $\text{Cl}^-$  anions and four methanol molecules. A perspective view of the binuclear entities with the atom-numbering scheme is depicted in Fig. 1. Crystallographic data are collected in Table 1 and selected bond lengths and angles are listed in Table 2.

Each diiron(III) complex cation is centrosymmetric, with two six-coordinated Fe(III) atoms being bridged by two deprotonated methoxyl groups. The BMA ligand coordinates towards one iron atom in a tridentate mode forming two five-membered chelate rings, together with one  $\text{Cl}^-$  ion and two oxygen atoms from deprotonated methanols completing the Fe(III) octahedral geometry. The Fe– $\text{N}_{\text{alkylamin}}$  bond (2.246 Å) and the Fe–Cl bond (2.275 Å) are significantly longer than the Fe– $\text{N}_{\text{imidazolyl}}$  ones (average 2.082 Å) and the Fe– $\text{O}_{\text{methoxyl}}$  (average 1.968 Å), also the bond angles around Fe(III), for instances  $\text{O1–Fe1–O1A}$  ( $76.58^\circ$ ) and  $\text{N1–Fe1–Cl1}$  ( $100.22^\circ$ ), indicating a distorted octahedron. In the  $\text{Fe}_2\text{O}_2$  bridging moieties, which are strictly planar due to the centrosymmetry, the parameters of Fe–O–Fe angle ( $103.41^\circ$ ) and Fe...Fe distance (3.089 Å) fall within the ranges reported for other dialkoxo-bridged diiron(III) complexes.<sup>4,5,26–29</sup> In the crystal lattice,  $\text{Cl}^-$  ions and non-coordinated methanol molecules as

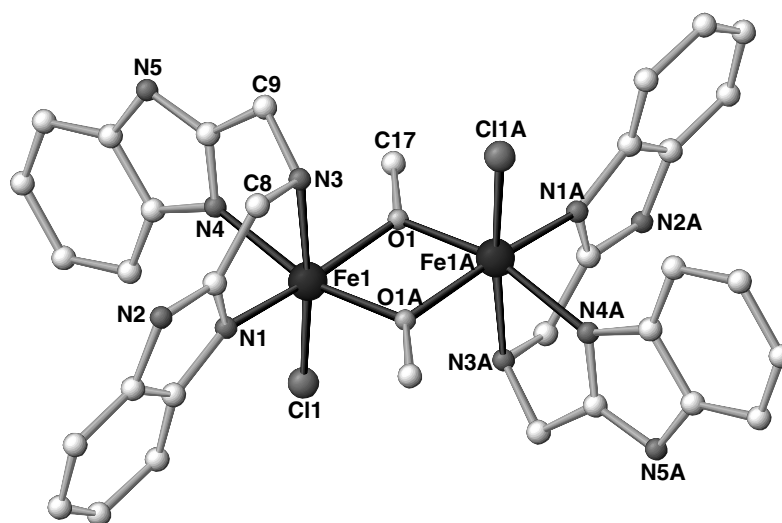


**Figure 1.** A perspective view of the binuclear cation in **1**.

**Table 1.** Crystallographic data for complex **1**

Formula	C <sub>38</sub> H <sub>52</sub> Cl <sub>4</sub> Fe <sub>2</sub> N <sub>10</sub> O <sub>6</sub>
Formula weight	998.40
Crystal system	Monoclinic
Space group	P2(1)/n
Unit cell dimensions	$a = 12.9659(19) \text{ \AA}$ $\alpha = 90.00^\circ$ $b = 10.0278(16) \text{ \AA}$ $\beta = 93.766(8)^\circ$ $c = 17.919(2) \text{ \AA}$ $\gamma = 90.00^\circ$
$V (\text{\AA}^3)$ , $Z$	2324.8(6), 2
$D_{\text{calc}} (\text{g cm}^{-3})$	1.426
$\mu (\text{mm}^{-1})$	0.908
$T (\text{K})$	293(2)
$F(000)$	1036
Crystal size (mm)	$0.35 \times 0.25 \times 0.20$
$\theta$ range for data collection (deg)	$2.00\text{--}26.39^\circ$
Limiting indices	$-16 \leq h \leq 16, 0 \leq k \leq 12, 0 \leq l \leq 22$
Unique reflections	4696 [ $R(\text{int}) = 0.0502$ ]
Max. and min. transmission	0.7417 and 0.8393
Refinement method	Full-matrix least-squares on $F^2$
Data/restraints/parameters	4696/0/276
Goodness-of-fit on $F^2$	1.009
Final $R$ indices [ $I > 2\sigma(I)$ ]	$R^1 = 0.0534, wR^2 = 0.1148$
$R$ indices (all data)	$R^1 = 0.1051, wR^2 = 0.1335$
Largest peak and hole ( $\text{e \AA}^{-3}$ )	0.656 and $-0.578$

**Table 2.** Bond lengths ( $\text{\AA}$ ) and angles (deg) for complex **1**

Fe1–O1A	1.962(3)	Fe1–N4	2.092(3)
Fe1–O1	1.974(3)	Fe1–N3	2.246(3)
Fe1–N1	2.072(3)	Fe1–Cl1	2.275(1)
O1A–Fe1–O1	76.59(3)	N1–Fe1–Cl1	100.20(8)
O1A–Fe1–N1	161.54(1)	N4–Fe1–Cl1	98.29(9)
O1–Fe1–N1	93.57(1)	N3–Fe1–Cl1	174.69(8)
O1A–Fe1–N4	94.95(1)	N1–Fe1–N3	77.38(1)
O1–Fe1–N4	162.52(1)	N4–Fe1–N3	77.09(1)
N1–Fe1–N4	90.07(2)	O1A–Fe1–Cl1	96.65(8)
O1A–Fe1–N3	86.43(1)	O1–Fe1–Cl1	97.88(8)
O1–Fe1–N3	87.03(1)	Fe1A–O1–Fe1	103.41(2)

Symmetry transformations used to generate equivalent atoms:  $A -x + 1, -y + 1, -z + 1$ .

### Spectroscopic characterization

The IR spectra of the title complex display the characteristic bands of the BMA ligand. The  $\nu(\text{C}=\text{N})$  absorption of the benzimidazole is observed at  $1620 \text{ s cm}^{-1}$ , and  $\nu(\text{C}-\text{N})$  at  $1450 \text{ s cm}^{-1}$ , and they are slightly shifted to higher wavenumbers than those of free ligand. The wide bands in the range of  $3100\text{--}3400 \text{ cm}^{-1}$  can be assigned to the  $\nu(\text{OH})$  stretching frequency and the sharp band of  $\nu(\text{N}-\text{H})$  is at  $3350 \text{ cm}^{-1}$ . The absorption bands, near  $900 \text{ w cm}^{-1}$  and  $740 \text{ m cm}^{-1}$ , are due to out-of-plane bend vibration correlating with aryl ring, where s, m and w refer to strong, medium and weak, respectively. The electronic spectrum of the complex in methanol shows three very strong absorptions at  $206 \text{ nm}$  ( $\epsilon = 5.67 \times 10^4 \text{ l mol}^{-1} \text{ cm}^{-1}$ ),  $272 \text{ nm}$  ( $\epsilon = 4.69 \times 10^4 \text{ l mol}^{-1} \text{ cm}^{-1}$ ) and  $278 \text{ nm}$  ( $\epsilon = 4.54 \times 10^4 \text{ l mol}^{-1} \text{ cm}^{-1}$ ), which may be attributed to charge transfer and the transition of the ligand itself. In addition, a weak broad band around  $441 \text{ nm}$  ( $\epsilon \approx 3262 \text{ l mol}^{-1} \text{ cm}^{-1}$ ) may be observed in the concentrated solution. According to ligand field theory and

well as the NH groups of BMA ligand form wide hydrogen bonds. The relevant distances and angles of the hydrogen bonds are also given in Table 3.

**Table 3.** Hydrogen bonds with  $H \cdots A < r(A) + 2.000 \text{ \AA}$  and  $DHA > 110^\circ$ 

D–H	d(D–H)	d(H···A)	<DHA	d(D···A)	A
N2–H2B	0.860	1.810	173.43	2.666	O3[ $-x + 1/2, y - 1/2, -z + 1/2$ ]
N3–H3B	0.910	2.416	161.86	3.293	Cl1[ $-x + 1, -y + 1, -z + 1$ ]
N5–H5B	0.860	1.965	163.90	2.801	O2
O2–H2	0.820	2.299	154.60	3.060	Cl2
O3–H3	0.820	2.228	172.17	3.042	Cl2

assuming  $O_h$  symmetry, the ground state of the distorted octahedron Fe(III) is  ${}^6A_{1g}$ . This band can be tentatively attributed to the overlap peak of multifold electronic transitions:  ${}^6A_{1g} \rightarrow {}^4T_{2g}(G)$  and  ${}^6A_{1g} \rightarrow {}^4A_{1g}({}^4E_g(G))$  and  ${}^6A_{1g} \rightarrow {}^4T_{2g}(D)$ .<sup>30–32</sup>

### ESR and magnetic properties

In the ESR spectrum, the sharp signal observed at  $g = 4.27$  ( $S = 5/2$ ) and the signal at  $g = 2.01$  ( $S = 1/2$ ) are characteristic of a high-spin non-heme ferric system, and the signal at  $g = 6.78$  is due to Fe(III) with axial symmetry, which accorded with the result of magnetic measure. High-spin octahedral Fe(III) complexes normally exhibit  $g$  values close to free spin in their ESR spectra, but highly distorted six-coordinate environments are known to result in large values (such as  $g = 8.88$ ).<sup>33,34</sup>

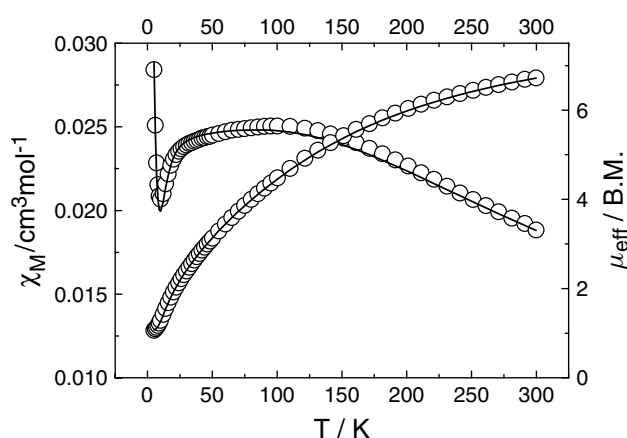
Variable-temperature magnetic susceptibilities for **1** were measured in the 4.2–300 K temperature range and are shown as  $\chi_M$  and  $\mu_{\text{eff}}$  vs  $T$  plots in Fig. 2. The experimental  $\mu_{\text{eff}}$  value at room temperature is ca. 6.72 B.M., well below the spin-only value (8.36 B.M.) expected for an uncoupled diiron(II) unit. Upon cooling, the magnetic moment declines monotonically until 10 K. These features, together with the temperature dependence behavior of  $\chi_M$  above 10 K, are characteristic of an antiferromagnetic interaction between the Fe(III) ions. On further cooling, the  $\mu_{\text{eff}}$  vs  $T$  plot reaches an approximate plateau, with the magnetic moment in the 1.28–1.06 B.M. range, while the  $\chi_M$  value increases sharply. This low-temperature behavior indicates the presence of small quantities of paramagnetic impurities.<sup>35–37</sup>

For diiron(III) complexes ( $S_1 = S_2 = 5/2$ ), the theoretical expression of the magnetic susceptibility based on  $\hat{H} = -2J\hat{S}_1\hat{S}_2$  is:

$$\chi_{bi} = \frac{2Ng^2\beta^2}{KT} \left[ \frac{55 \exp(\frac{15J}{KT}) + 30 \exp(\frac{10J}{KT}) + 14 \exp(\frac{6J}{KT}) + 5 \exp(\frac{3J}{KT}) + \exp(\frac{J}{KT})}{1 + 9 \exp(\frac{10J}{KT}) + 7 \exp(\frac{6J}{KT}) + 5 \exp(\frac{3J}{KT}) + 3 \exp(\frac{J}{KT}) + 11 \exp(\frac{15J}{KT})} \right]$$

$$\chi = \chi_{bi}(1 - \rho) + \frac{2Ng^2\beta^2}{3KT} \cdot S(S+1) \cdot \rho$$

where  $J$  is the exchange integral between Fe(III) ions bridged by methoxyl oxygen atoms,  $\rho$  accounts for

**Figure 2.** Plots of  $\chi_M$  and  $\mu_{\text{eff}}$  vs  $T$  for complex **1**.

paramagnetic impurities [presumably monomeric high-spin Fe(III) complex,  $s = 5/2$ ], and the other parameters have their usual meanings. An isotropic  $g$  value of 1.99 was assumed. The simulation of experimental data leads to  $J = -27.05 \text{ cm}^{-1}$ ,  $\rho = 0.003$ ,  $R = \sum (\chi_{\text{obsd}} - \chi_{\text{calcd}})^2 / \sum \chi_{\text{obsd}}^2 = 1.92 \times 10^{-4}$ .

The above  $J$  value, which near to the range ( $-2.5$  to  $-25 \text{ cm}^{-1}$ ) observed for other dialkoxo- or dihydroxo-bridged diiron(III) complexes, suggests a moderate antiferromagnetic exchange between iron(III) ions. The magnetic interaction is somewhat stronger than those diiron complexes in literature, maybe resulting from somewhat its shorter Fe···Fe distance, a smaller bridging angle and comparable Fe–O distances in complex **1**.<sup>38</sup> However, it has been reported that the interaction magnitude in oxo-, hydroxo- or alkoxo-bridged diiron(III) complexes is quite insensitive to the bridging angle and the Fe···Fe distance.<sup>39</sup>

### Plasmid–complex1 binding studies

#### Electronic spectral method

As shown in Fig. 3, the potential pBR322 DNA binding ability of complex **1** was studied by UV spectroscopy. To obtain practical DNA-mediated hypochromic spectra of the diiron complex absorption, absorption spectra of the diiron complex in the absence and the presence of DNA were performed, respectively, involving different molar concentration ratios of DNA to the diiron complex from 0:1 to 12:1 in 10 mM pH 7.5 Tris–Cl buffer. The result shows decreases in the peak intensity of the intraligand  $\pi \rightarrow \pi^*$  transition band at  $\sim 209 \text{ nm}$

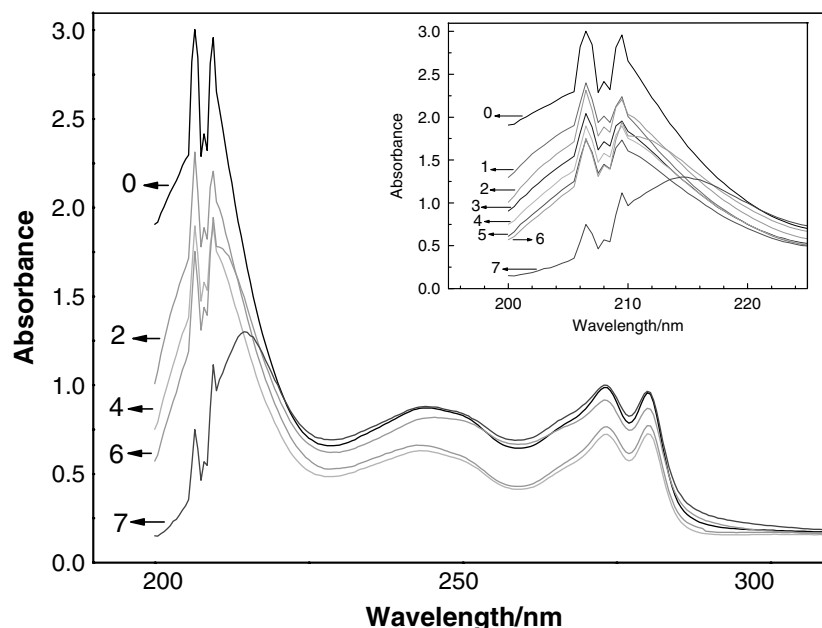


**Figure 3.** Absorption spectra of **1** (20  $\mu\text{M}$ ) with increasing the molar concentration ratio of DNA to the diiron complex of 0 : 1 (line 0), 1 : 1 (line 1), 2 : 1 (line 2), 3 : 1 (line 3), 4 : 1 (line 4), 5 : 1 (line 5), 6 : 1 (line 6) and 12 : 1 (line 7) in 10 mM pH 7.5 Tris–Cl buffer.

and a slight red shift ( $\sim 5$  nm) along with increasing amounts of pBR322 DNA. The hypochromism was suggested to be commonly due to a moderate interaction of a complex bound to DNA through intercalation.<sup>40–44</sup>

### Gel electrophoretic method

The ability of  $[\text{Fe}_2(\text{BMA})_2(\text{CH}_3\text{O})_2\text{Cl}_2] \cdot 2\text{Cl} \cdot 4\text{CH}_3\text{OH}$  to perform DNA cleavage under physiological conditions (pH 7.5, 37  $^\circ\text{C}$ ) was observed by the transformation of the supercoiled form (form I) to the nicked form (form II) of plasmid DNA. Figure 4 shows the cleavage status of pBR322 DNA mediated by complex **1** with various concentrations. It is clear from lanes 1–4 that the diiron complex exhibits the trend that increasing concentration results in more efficient cleavage. The results accorded with the literature and study of the mechanism of DNA cleavage activity by the diiron complex is under way.



**Figure 4.** Agarose gel electrophoresis of pBR322 DNA (0.8  $\mu\text{g}$ ) cleavage by **1** in a buffer containing 10 mM Tris, 1 mM  $\text{Na}_2\text{EDTA}$  and HCl (adjusted pH = 7.5) at 37  $^\circ\text{C}$  for 3 h. Lanes 1–5, with 1.00, 0.50, 0.25, 0.05 and 0.00 mM of **1** added (lane 5: blank DMSO contrast).

### Acknowledgments

This work was supported by the National Natural Science Foundation of China (no. 20331020), Tianjin Natural Science Foundation, China (no. 06YFJMJC12700) and Tianjin University Committee Science Foundation, China (no.20020106).

### REFERENCES

- Mukherjee RN, Stack TDP, and Holm R. *J. Am. Chem. Soc.* 1988; **110**: 850.
- Tatsumi K, Hoffmann R. *J. Am. Chem. Soc.* 1981; **103**: 3328.
- Andersson KK, Graslund A. *Adv. Inorg. Chem.* 1996; **43**: 359.
- Solomon EI, Brunold TC, Davis MZ, Kemsley JN, Lee S-K, Lehnert N, Skulan AJ, Yang YS, Zhou J. *Chem. Rev.* 2000; **100**: 235.
- Waller BJ, Lipscomb JD. *Chem. Rev.* 1996; **96**: 2625.
- Feig AL, Lippard SJ. *Chem. Rev.* 1994; **94**: 759.
- Stenkamp RE. *Chem. Rev.* 1994; **94**: 715.
- Rosenzweig AC, Nordlund P, Takahara PM, Frederick CA, Lippard SJ. *Chem. Biol.* 1995; **2**: 409.
- Kurtz DM Jr. *J. Biol. Inorg. Chem.* 1997; **2**: 159.
- Nordlund P, Sjöberg B-M, Eklund H. *Nature* 1990; **345**: 593.
- Sträter N, Klabunde T, Tucker P, Witzel H, Krebs B. *Science* 1995; **268**: 1489.
- Hegg EL, Burstyn JN. *Coord. Chem. Rev.* 1998; **173**: 133.
- Liu CL, Yu SW, Li DF, Liao ZR, Sun XH, Xu HB. *Inorg. Chem.* 2002; **41**: 913.
- Fu PKL, Bradley PM, Turro C. *Inorg. Chem.* 2001; **40**: 2467.
- Sissi C, Rossi P, Felluga F, Formaggio F, Palumbo M, et al. *J. Am. Chem. Soc.* 2001; **123**: 3169.
- Wilhelmsson LM, Westerlund F, Lincoln P, Norden B. *J. Am. Chem. Soc.* 2002; **124**: 12092.
- Verge F, Lebrun C, Fontecave M, Menage S. *Inorg. Chem.* 2003; **42**: 499.
- Radzicka A, Wolfenden R. *Science* 1995; **267**: 90.

19. Sreedhara A, Freed JD, Cowan JA. *J. Am. Chem. Soc.* 2000; **122**: 8814.
20. Zhu B, Zhao DQ, Ni JZ, Zeng QH, Huang BQ, Wang ZL. *Inorg. Chem. Commun.* 1999; **2**: 351.
21. McCue KP, Morrow JR. *Inorg. Chem.* 1999; **38**: 6136.
22. Sigman DS, Chen CHB. *A. Rev. Biochem.* 1990; **59**: 207.
23. Basile LA, Barton JK. *J. Am. Chem. Soc.* 1987; **109**: 7548.
24. Xu J-Y, Gu W, Li L, Yan SP, Cheng P, Liao D-Z, Jiang Z-H. *J. Mol. Struct.* 2003; **644**(1–3): 23.
25. Sheldrick GM. *SHELXS-97 and SHELXL-97, Software for Crystal Structure Analysis*. Siemens Analytical X-ray Instruments: Wisconsin, MA, 1997.
26. Wu CHS, Rossman GR, Gray HB, Hammond GS, Schugar HJ. *Inorg. Chem.* 1972; **11**: 990.
27. Bertrand JA, Breece JL, Eller PG. *Inorg. Chem.* 1974; **13**: 125.
28. Nishida Y, Takeuchi M, Shimo H, Kida S. *Inorg. Chim. Acta* 1984; **90**: 115.
29. Yin L, Cheng P, Yao X, Wang H. *J. Chem. Soc. Dalton. Trans.* 1997; 2109.
30. Allen GC, El-Sharkawy GAM, K. Warren D. *J. Chem. Soc. Dalton. Trans.* 1971; **10**: 2538.
31. Birchall T, Greenwood NN, Reid AF. *J. Chem. Soc. Dalton. Trans.* 1969; 2382.
32. Lever ABP. *Inorganic Electronic Spectroscopy*. Elsevier: Amsterdam, 1968; Chapter 9.
33. Constable EC, Ward MD, Tocher DA. *J. Chem. Soc., Dalton Trans.* 1991; 1675.
34. Neto LM, Tabak M, Nascimento OR. *J. Inorg. Biochem.* 1990; **40**: 309.
35. Wollmann RG, Hendrickson DN. *Inorg. Chem.* 1977; **16**: 723.
36. Wahlgren CG, Addison AM, Burman S, Thompson LK, Sinn E, Rowe TM. *Inorg. Chim. Acta* 1989; **166**: 59.
37. Arulsamy N, Hodgson DJ, Glerup J. *Inorg. Chim. Acta* 1993; **209**: 61.
38. Gao E-Q, Yin L-H, Tang J-K, Cheng P, Dai D-Z, Jiang Z-H, Yan S-P. *Polyhedron* 2001; **20**: 669.
39. Hotzelmann R, Wieghardt K, Flörke U, Haupt H-J, Weatherburn DC, Bonvoisin J, Blondin G, Girerd J-J. *J. Am. Chem. Soc.* 1992; **114**: 1681.
40. Long EC, Barton JK. *Acc. Chem. Res.* 1990; **23**: 271.
41. Uma V, Kanthimathi M, Weyhermuller T. *J. Inorg. Biochem.* 2005; **99**: 2299.
42. Selvakumar B, Rajendiran V, Maheswari PU, Evans HS, Palaniandavar M. *J. Inorg. Biochem.* 2006; **100**: 316.
43. Berman HM, Young PR. *A. Rev. Biophys. Bioengng* 1981; **10**: 87.
44. Cantor C, Schimmel PR. *Biophysical Chemistry*, Vol. 2. Freeman: San Francisco, CA, 1980; 398.